Aggregates of scrapie-associated prion protein induce the cell-free conversion of protease-sensitive prion protein to the protease-resistant state

Byron Caughey[1]*, David A Kocisko[1,2], Gregory J Raymond[1] and Peter T Lansbury, Jr[2]*

[1]Laboratory of Persistent Viral Diseases, Rocky Mountain Laboratory, NIAID, NIH, Hamilton, MT 59840, USA and [2]Department of Chemistry, Massachusetts Institute of Technology, Cambridge, MA 02139, USA

Introduction: Scrapie infection instigates the *in vivo* conversion of normal, protease-sensitive prion protein (PrP^C) into a protease-resistant form (PrP^{Sc}) by an unknown mechanism. *In vitro* studies have indicated that PrP^{Sc} can induce this conversion, consistent with proposals that PrP^{Sc} itself might be the infectious scrapie agent. Using this cell-free model of the PrP^C to PrP^{Sc} conversion, we have studied the dependence of conversion on reactant concentration, and the properties of the PrP^{Sc}-derived species that has converting activity.

Results: The cell-free conversion of ^{35}S PrP^C to the proteinase K-resistant form was dependent on the reaction time and initial concentrations of PrP^{Sc} (above an apparent minimum threshold concentration) and ^{35}S PrP^C. Analysis of the physical size of the converting activity indicated that detectable converting activity was associated only with aggregates. Under mildly chaotropic conditions, which partially disaggregated PrP^{Sc} and enhanced the converting activity, the active species were heterogeneous in size, but larger than either effectively solubilized PrP or molecular weight standards of ~2000 kDa.

Conclusions: The entity responsible for the converting activity was many times larger than a soluble PrP monomer and required a threshold concentration of PrP^{Sc}. These results are consistent with a nucleated polymerization mechanism of PrP^{Sc} formation and inconsistent with a heterodimer mechanism.

Chemistry & Biology December 1995, **2**:807–817

Key words: scrapie, prion protein, aggregation, *in vitro* formation, sedimentation

Introduction

The transmissible spongiform encephalopathies (TSEs or prion diseases) include Creutzfeldt–Jakob disease, Gerstmann–Straussler disease and kuru in humans, scrapie in sheep, mice and hamsters, and bovine spongiform encephalopathy (for review see [1]). These neurodegenerative diseases are characterized by the accumulation of abnormal protease-resistant forms of the prion protein (PrP), for example PrP^{Sc}, in diseased animals. PrP^{Sc} forms insoluble aggregates (e.g., amyloid plaques) and is partially resistant to proteinase K (PK) [2–4], which removes only ~67 amino acid residues (6–7 kDa) from the amino terminus of each residual molecule in the aggregates [5,6]. In contrast, the normal, non-pathogenic form, PrP^C, is soluble in mild detergents and fully degraded by PK [7,8]. PrP^C has been shown to be the precursor of PrP^{Sc} [9,10]. No covalent difference has been detected between PrP^C and PrP^{Sc} that explains their differences in aggregation properties and protease sensitivity [6,11].

Although infectivity has not been separated from PrP^{Sc} [12,13], the exact makeup of the infectious agent remains speculative. One school of thought initiated by Griffith in 1967 [14] postulates that the agent is a pathogenic form of a host protein which, upon entering a new host, can induce the conversion of a normal endogenous protein to more of the pathogenic form [14–16]. The inability to separate PrP^{Sc} and scrapie infectivity has made PrP^{Sc} the prime candidate for this putative infectious protein agent [12,13,16]. Supporting this model are observations that PrP^C will convert to PK-resistant forms when incubated with preexisting PrP^{Sc} in a cell-free system (Fig. 1) [17–19]. It is not yet known whether new scrapie infectivity is generated upon conversion of PrP^C to these PK-resistant forms. Further biochemical studies with this cell-free system have shown, however, that there is scrapie-strain and PrP-species specificity in the PrP^C–PrP^{Sc} interactions that could account for the observed differences between scrapie strains and the barriers to interspecies transmission of scrapie, respectively [18,19]. The precise nature and mechanism of the activity within PrP^{Sc} preparations that converts PrP^C to protease-resistant PrP is not well defined.

Any mechanistic model for PrP^{Sc} formation must address two questions regarding the conversion reaction. First, what catalyzes the conversion of PrP^C to PrP^{Sc} (the 'converting activity')? Two distinct models have been proposed for how this occurs. According to the heterodimer/unfolding model, the catalyst (PrP^{Sc}) is a monomeric conformational

*Corresponding authors.

 ISSN 1074-5521

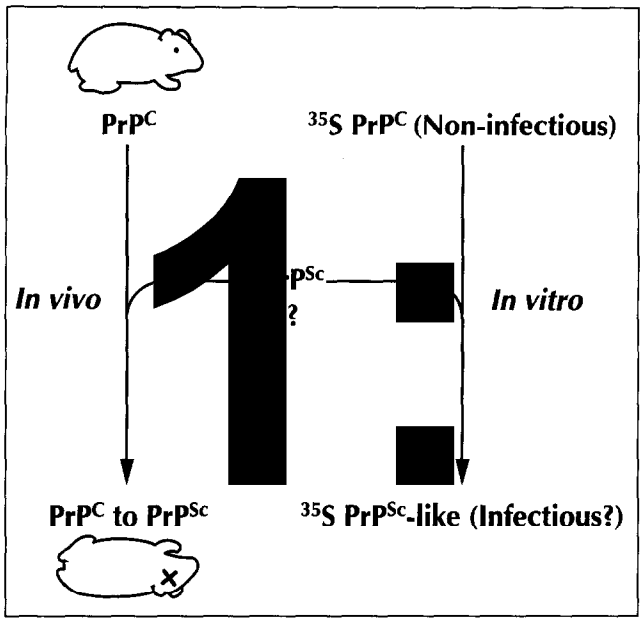

Fig. 1. A possible analogy between the *in vitro* conversion of PrP^C to PrP^{Sc}-like, PK-resistant forms, and scrapie infection *in vivo*. The *in vitro* system mimics *in vivo* infection in that protease-resistant PrP is produced by a mechanism that exhibits host-species and scrapie-strain specificities, but the generation of new scrapie infectivity remains to be demonstrated.

isomer of PrP that catalyzes the conformational change via a PrP^C–PrP^{Sc} heterodimer [14–16]. Alternatively, the nucleation model holds that the catalyst is an ordered multimeric aggregate of PrP (PrP^{Sc}) which acts as a seed for polymerization of PrP [20,21]. Second, what is the barrier that prevents the spontaneous conversion of PrP^C to PrP^{Sc}? The heterodimer/unfolding model holds that the barrier is the activation energy for the conformational change in PrP^C. In the nucleation model, the barrier is the unfavorable formation of a multimeric nucleus. TSE infection would then bypass nucleus formation by providing preformed PrP^{Sc} seeds.

Attempts to determine the mechanism of PrP^{Sc} formation are complicated by the fact that the reaction itself and the physical state of PrP^{Sc} are difficult to monitor *in vivo*. The *in vitro* system described above does, however, allow direct characterization of the species capable of inducing the conversion of PrP^C to PrP^{Sc}-like protease-resistant forms. Here we describe experiments assessing the dependence of the conversion reaction on the concentration of the reactants and the determination of the size of the molecular species associated with converting activity by sedimentation and ultrafiltration analysis.

Results

Concentration dependence of the cell-free conversion of ^{35}S PrP^C to the protease-resistant form

The extent of conversion of ^{35}S PrP^C to protease-resistant, PrP^{Sc}-like species was followed as a function of time and the amount of PrP^{Sc} added to the reaction mixture (Fig. 2a, b). In this reaction, ^{35}S PrP^C immunoprecipitated from uninfected fibroblast cells was mixed with scrapie-brain-derived PrP^{Sc} in 2.5 M guanidine–HCl (GdnHCl) and then diluted to 0.75 M GdnHCl to initiate the conversion reaction. After the incubation period, the products of the reaction were treated with PK to test for the conversion of ^{35}S PrP^C to PK-resistant forms. For quantitative comparisons throughout this study, 'conversion' was defined as the formation of 16–20 kDa PK-resistant ^{35}S PrP, since this is the size expected for PK-digested PrP^{Sc} derived from this type of PrP^C precursor [17,22] (6–7 kDa lower in molecular weight than the full length 23–27 kDa precursor; see also Fig. 4a). Figure 2b illustrates the increase in conversion as either the initial concentration of PrP^{Sc} or the incubation period were increased.

The extent of conversion at 22 h was then determined over a wider range of PrP^{Sc} concentrations (Fig. 2c). Increasing the concentration of PrP^{Sc} always increased the extent of conversion, although at high concentrations of PrP^{Sc} ($\gtrsim 100\ \mu g\ ml^{-1}$) the concentration dependence was less marked. At concentrations of PrP^{Sc} from 8 to 62 $\mu g\ ml^{-1}$, a plot of percent conversion versus initial concentration of PrP^{Sc} was essentially linear (Fig. 2d). Extrapolation of such a plot to percent conversion = 0 resulted in a non-zero x-intercept (~5.1 $\mu g\ ml^{-1}$ or 150 nM), providing evidence that a threshold concentration of PrP^{Sc} was required for the existence of converting activity (see below). Further, conversion attempted with 2 or 4 $\mu g\ ml^{-1}$ PrP^{Sc} gave no detectable conversion product (data not shown). The observed threshold concentration probably depends upon the presence of GdnHCl and thus may be different (presumably lower) in the absence of GdnHCl. The dependence of the total conversion at 22 h on the concentration of ^{35}S PrP^C was also determined (Fig. 2e). At a constant concentration of PrP^{Sc} (125 $\mu g\ ml^{-1}$), the formation of ^{35}S-labeled conversion product was directly dependent on the initial concentration of ^{35}S PrP^C. Extrapolation to 0% conversion demonstrated no threshold PrP^C concentration. Note, however, that, due to the limited availability of PrP^C, the range of concentrations of ^{35}S PrP^C examined was ~1% of the range of PrP^{Sc} concentrations tested in Fig. 2b (see Materials and methods).

Sedimentation properties of the converting activity

We have reported that pretreatment of PrP^{Sc} with 3 M GdnHCl enhances the converting activity [17]. Subsequently, we have found that the optimal pretreatment concentration varies from 2 to 3 M GdnHCl depending upon the particular PrP^{Sc} preparation (data not shown). Such GdnHCl treatments are also known to partially disaggregate PrP^{Sc} [23,24]. To determine whether converting activity was associated with a solubilized PrP^{Sc} fraction or a residual PrP^{Sc} aggregate, we analyzed the sedimentation properties of the converting activity in the presence of GdnHCl. Treatments with GdnHCl can alter the biochemical properties (i.e. PK resistance and tendency to aggregate) of PrP^{Sc} that are usually used to define PrP^{Sc} and distinguish it from PrP^C. Nonetheless, to define the origin of samples derived from

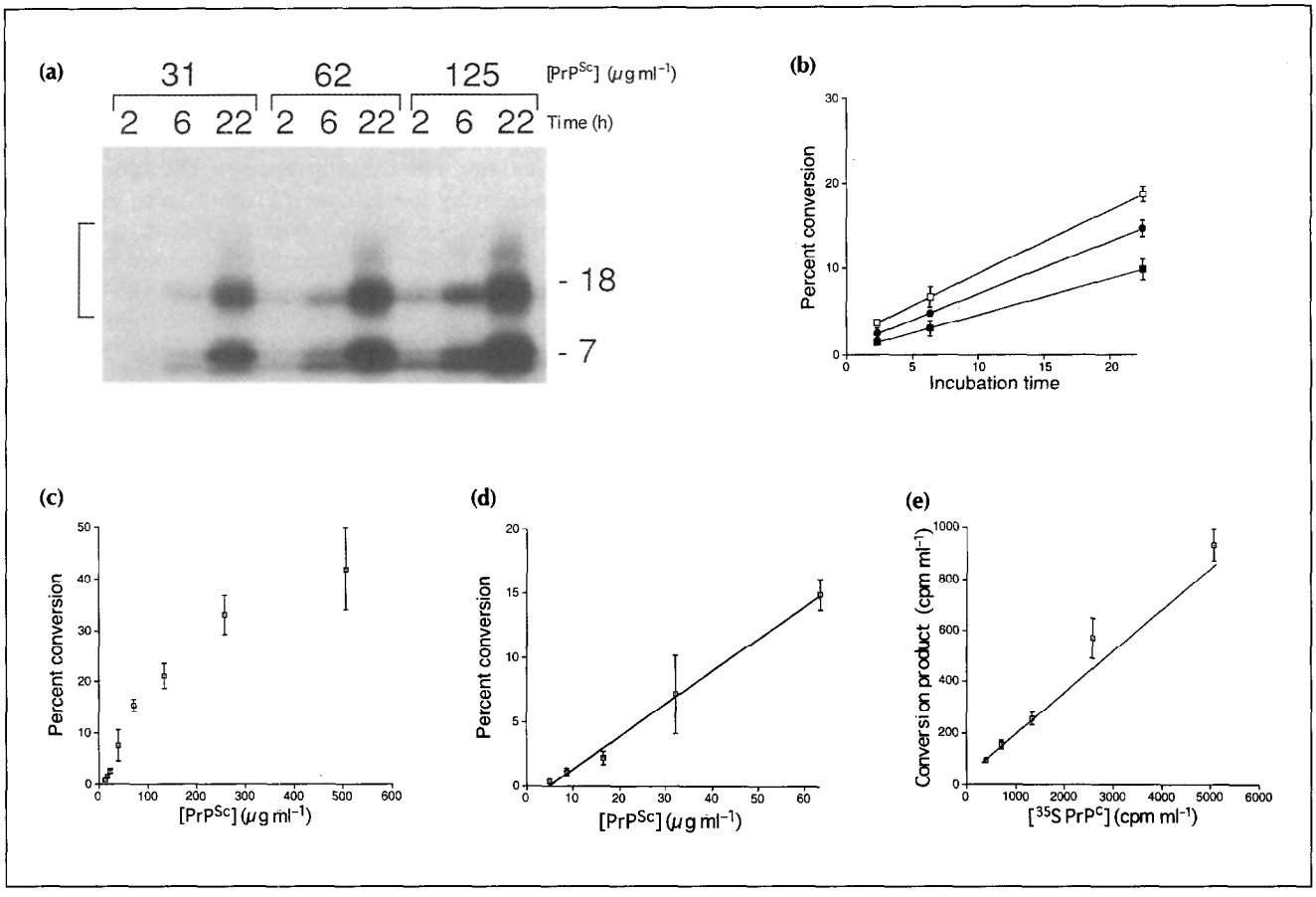

Fig. 2. The conversion reaction is dependent on the time of incubation and the concentrations of PrP^{Sc} and ^{35}S PrP^{C}. **(a)** Converting activity. PK-resistant ^{35}S PrP species generated from the incubation of ^{35}S PrP^{C} with different concentrations of PrP^{Sc} (μg ml^{-1}) for various lengths of time (h) as described for the conversion reaction in Materials and methods. The PrP^{C} used in this study lacks a GPI anchor and is predominantly unglycosylated (23 kDa), with a minority monoglycosylated (27 kDa) species (see Fig. 4a, for example). The bracket on the left and in subsequent figures indicates the PrP^{Sc}-like 16–20 kDa bands that were used in the quantitative comparisons described below. All lanes represent reactions initiated with 60 000 cpm of ^{35}S PrP^{C}. Molecular weight markers are indicated at the right in kDa. **(b)** Percent of ^{35}S PrP^{C} converted to 16–20 kDa PK-resistant species (mean +/– standard deviation of triplicate determinations) after incubation with designated PrP^{Sc} concentrations as a function of incubation time (includes data shown in (a)). Only bracketed bands as shown in (a) were counted as converted product using the Phosphorimager. □, 125 μg ml^{-1}; ●, 62 μg ml^{-1}; ■, 31 μg ml^{-1} **(c)** Percent conversion in 22 h versus PrP^{Sc} concentration. **(d)** Expanded plot of linear region of data in panel (c) showing a line fit by simple linear regression with an x-intercept of 5.1 μg ml^{-1} (150 nM PrP^{Sc}, based on a molecular weight of 35 kDa). **(e)** Plot of the total 16–20 kDa conversion product versus the initial concentration of ^{35}S PrP^{C}. Semi-quantitative immunoblotting was used to estimate the total PrP^{C} as 10 ng per 60 000 cpm. The concentration of PrP^{Sc} and incubation time were constant in these reactions at 125 μg ml^{-1} and 22 h, respectively. The percentage of the initial ^{35}S PrP^{C} that was converted was ~20% over the entire range tested.

PrP^{Sc} preparations, we will continue to refer to them as PrP^{Sc}, realizing that the PrP in these samples might no longer have the properties originally used to define PrP^{Sc}.

PrP^{Sc} pretreated with 3 M GdnHCl was centrifuged under conditions predicted to pellet 90% of particles that have a sedimentation coefficient at 20°C in water, $s_{20,w} = 12$ (based on calculations described in Materials and methods). The pellet and supernatant fractions were tested for converting activity (Fig. 3a) and analyzed for PrP content (without PK treatment) by immunoblotting (Fig. 3b). The vast excess of PrP^{Sc} over PrP^{C} in the reaction dictates that the PrP detected by immunoblot was derived predominantly from PrP^{Sc}. A majority of the PrP was found in the supernatant, but converting activity was found only in the pellet. This indicated that, although the 3 M GdnHCl treatment effectively solubilized more than half of the original PrP^{Sc} preparation and increased the overall converting activity [17], only sedimentable aggregates had converting activity.

To further compare the sedimentation rates of the entity responsible for converting activity and of GdnHCl-solubilized PrP^{Sc}, a series of sedimentation velocity centrifugations was performed (Fig. 4). In this experiment, PrP^{Sc} pretreated in 2.5 M GdnHCl was used because preliminary experiments with this particular PrP^{Sc} preparation indicated that the converting activity was optimal with this pretreatment (see below). The sample was placed over a layer of 5% sucrose in 2.5 M GdnHCl and centrifuged at various speeds. Fractions of the gradient were tested for converting activity (Fig. 4a, d) and analyzed by immunoblotting for total PrP content (Fig. 4b). With spins of 2000 and 8000 g, a majority of the converting activity

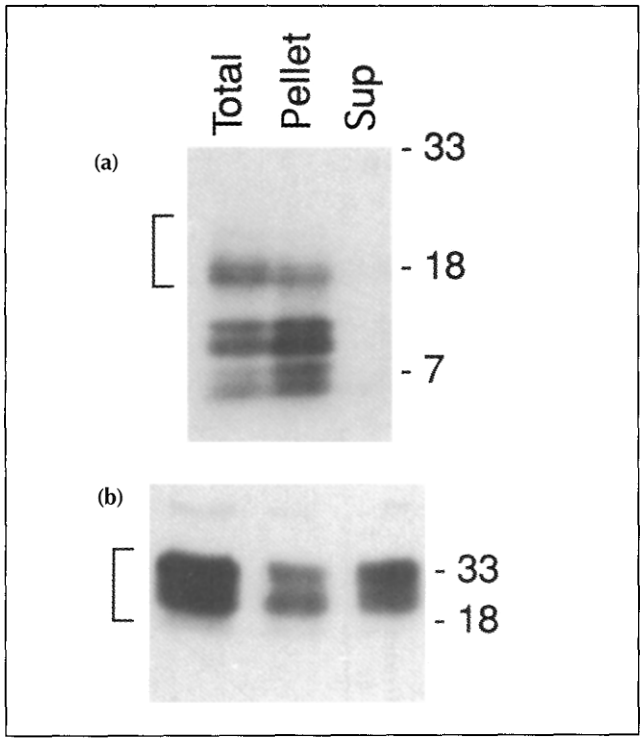

Fig. 3. The converting activity can be pelleted. **(a)** Converting activity (as described in legend to Fig. 2a) in aliquots of unseparated (total) PrP^{Sc} in 3 M GdnHCl or of pellet or supernatant (Sup) fractions of the same after centrifugation at 217 000 g max. **(b)** Immunoblot showing relative total PrP content of the same fractions used in the conversion reaction in (a). A polyclonal rabbit antiserum raised against a synthetic peptide corresponding to hamster PrP residues 90–104 was used [47]. Molecular weight markers are indicated at the right in kDa.

remained in the top (T) fraction corresponding to the sample zone (Fig. 4a, d). A spin at 70 000 g cleared > 95% of converting activity from the sample zone (T). Calculations based on the clearing factor (k) for this rotor speed and sample zone radius estimated that 90% of particles of $s_{20,w} = 17$ would be cleared from the sample zone under these conditions. A 234 000 g spin cleared all detectable converting activity from both the sample zone and middle (M) fractions. At this speed, ≥ 90% of particles of $s_{20,w} \geq 5$ would be cleared from the sample zone. In contrast to the converting activity, at least half of the PrP detected by immunoblot remained in the top (sample) zone after these spins (Fig. 4b). This confirmed that the detectable converting activity was associated with sedimentable aggregates rather than with the non-sedimenting PrP^{Sc} generated by the GdnHCl treatment.

A set of single-subunit molecular weight standard proteins (lactalbumin (14 kDa), trypsin inhibitor (20 kDa), carbonic anhydrase (30 kDa), ovalbumin (43 kDa), bovine serum albumin (67 kDa), and phosphorylase b (94 kDa); data not shown) and thyroglobulin (669 kDa, with 335 kDa subunits; Figure 4c) were centrifuged at 70 000 and 234 000 g in identical gradients containing 2.5 M GdnHCl, but none sedimented through the gradient to the extent observed for the converting activity at those centrifugal forces. Native thyroglobulin is 19 S, but the effect of 2.5 M GdnHCl on the sedimentation properties of thyroglobulin and the other protein molecular weight standards is not known. The sedimentation behavior of blue dextran (2000 kDa) was closest to that of the converting activity, but the clearance of the blue dextran absorbance from the sample (T) zone was still slower than that of the converting activity (Fig 4a, c, d). Thus, the detectable converting activity sedimented faster than the solubilized PrP (monomeric MW = 25–36 kDa), other proteins up to 335 kDa (if thyroglobulin subunits are dissociated in 2.5 M GdnHCl) and the 2000-kDa blue dextran.

To address the possibility that solubilization of converting activity might be achieved at a different GdnHCl concentration, PrP^{Sc} was treated in 0, 1.5, 2.0, 2.5 and 3.0 M GdnHCl and centrifuged at 234 000 g in gradients formed with a matching concentration of GdnHCl. In all cases, the detectable converting activity was cleared completely from the sample zone and sedimented to the bottom (B) and pellet (P) fractions (data not shown), indicating that the converting activity was associated with aggregates regardless of the GdnHCl concentration. GdnHCl concentrations greater than 3 M were not tested because, as noted above, converting activity is unstable at concentrations ≥ 3.5 M and not renaturable by subsequent dilution of the GdnHCl.

Sedimentation of PK-treated converting activity and PrP^{Sc}

Our treatment of PrP^{Sc} with PK results in the loss of approximately half of the total PrP and removal of 67 amino-terminal amino acids (6–7 kDa) from the remaining PrP^{Sc} to generate a predominantly 27–30 kDa protein (PrP 27–30) (Fig. 5; [5,6]). In addition, PK treatment degrades much of the large molecular weight (> 40 kDa) material that is observed by SDS-PAGE with typical PrP^{Sc} preparations (PrP 27–30 is > 90% pure as determined by SDS-PAGE [25]). Since PK treatment does not eliminate the converting activity associated with PrP^{Sc} [19], we tested whether PK pretreatment would allow the converting activity to be more readily disaggregated by GdnHCl. PrP 27–30 was treated with 2.5 M GdnHCl and subjected to a 234 000 g gradient centrifugation identical to that performed with the untreated PrP^{Sc} preparation. Analysis of the converting activity in the gradient fractions indicated that it pelleted (Fig. 6a) as it did prior to PK digestion (Figs. 3 and 4). Analysis of the total PrP by immunoblot indicated that, in contrast to the situation with the untreated PrP^{Sc}, none of the PrP 27–30 was effectively solubilized by the GdnHCl (Fig. 6b). This result suggested that PK digestion of PrP^{Sc} removed the PrP species that could be effectively solubilized from the PrP^{Sc} aggregates; it is the aggregates of PrP^{Sc} that are associated with converting activity in the presence of 2.5 M GdnHCl.

Ultrafiltration of converting activity in GdnHCl

As another test of the size of molecular species associated with converting activity, ultrafiltration was performed on

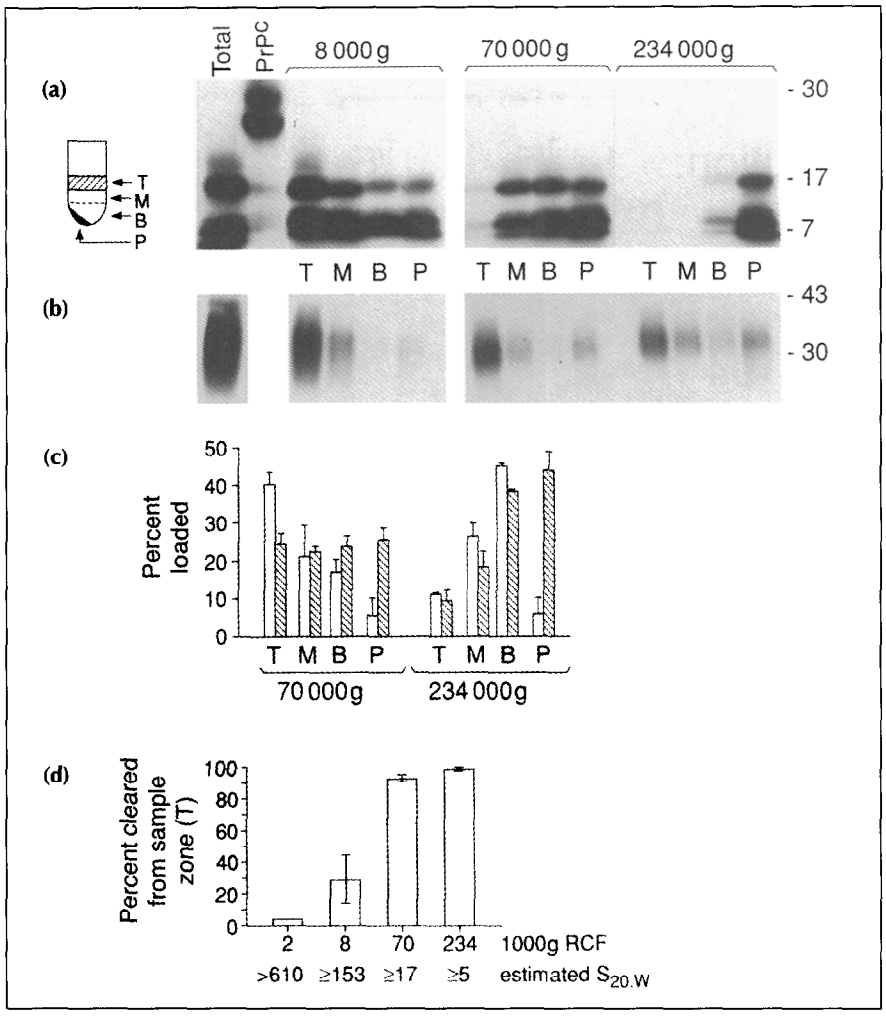

Fig. 4. Converting activity sediments more rapidly than both the majority of PrP^{Sc} protein and molecular weight standards up to 2000 kDa. **(a)** Converting activity (as described in legend to Fig. 2a) in aliquots of unfractionated (total) PrP^{Sc} in 2.5 M GdnHCl or top (T), middle (M), bottom (B), and pellet (P) fractions (as indicated by diagram at left) after centrifugation at the designated g force. One third of the ^{35}S PrP^{C} used in each conversion reaction is shown without PK digestion in the PrP^{C} lane. Molecular weight markers are indicated at the right in kDa. **(b)** Immunoblot of the total PrP in fractions described in (a). **(c)** Sedimentation of thyroglobulin (669 kDa total, 335 kDa subunits; clear bars) or blue dextran (2000 kDa; hatched bars) in 2.5 M GdnHCl on identical gradients. The data points show the percent of the amount loaded (mean +/– S.D.) in fractions from three gradients. **(d)** Clearance of the converting activity from the sample (T) zone after centrifugation at the designated relative centrifugal forces (RCF). The ordinate is the percent reduction in the conversion activity generated by aliquots of the T fractions as compared to the total unfractionated PrP^{Sc} sample. The data points show the mean +/– range of measurements from two independent experiments (including the one in (a)), except in the case of the 2000 g spin which is from a single determination. For comparison, the calculated $s_{20,w}$ values of particles that would be 90% cleared from the sample zone under the conditions of each centrifugation are shown.

PrP^{Sc} (not treated with PK) in 3 M GdnHCl. PrP^{Sc}-derived PrP was retained by a filter with a nominal molecular weight limit (NMWL) rating of 100 kDa (data not shown) but passed through a 300 kDa NMWL filter (Fig. 7b). In contrast, the converting activity was retained by the 300 kDa NMWL filter (Fig. 7a). Thus, the 300 kDa NMWL filter separated the converting activity from the bulk of the solubilized PrP^{Sc}, providing additional evidence that the converting activity is associated only with aggregates larger than the dissociated PrP. Since the maximum pore size of the 300 kDa NMWL filter is estimated by the manufacturer to be ~30 nm, the Stokes radius of the inactive PrP that passed through this filter would then be < 30 nm. The Stokes radius of the converting activity must be larger than that of the PrP^{Sc}-derived material without converting activity; however, one cannot definitively conclude that it is greater than 30 nm because of possible polarization layer effects and the likelihood that the average pore size of the filter is much lower than 30 nm.

Similar filtration experiments performed with filters with nominal maximum pore sizes of 100–450 nm indicated that converting activity could pass through the filters (data not shown). The passage of converting activity through the 100 nm (maximum pore size) filter indicated that under these conditions it can have a Stokes radius of ≤ 100 nm.

Ultrafiltration of PK-treated converting activity in GdnHCl

Ultrafiltration of PK-treated PrP^{Sc} in 3 M GdnHCl indicated that the converting activity was retained by both 100 and 300 kDa NMWL filters (Fig. 8a) as was the case with the untreated PrP^{Sc} (Fig. 7a). In contrast to the untreated PrP^{Sc}, little (<15%) of the PK-treated PrP^{Sc} passed through the 300 kDa NMWL filter (Fig. 8b). This was consistent with the sedimentation analysis of PK-treated PrP^{Sc} (Fig. 6b), which also indicated reduced solubilization by GdnHCl compared to the PrP^{Sc} that was not treated with PK.

Discussion

Association of converting activity with PrP^{Sc} aggregates

The recently developed cell-free reaction for converting PrP^{C} to PK-resistant forms has made it possible to begin to characterize the components and mechanism of the converting activity under defined conditions. The dependence of the conversion rate on the amount of PrP^{Sc} in the reaction mixture establishes that a component of the PrP^{Sc} preparation is involved in the rate-determining step. The sedimentation and filtration of the converting activity indicates that it is associated with aggregates that

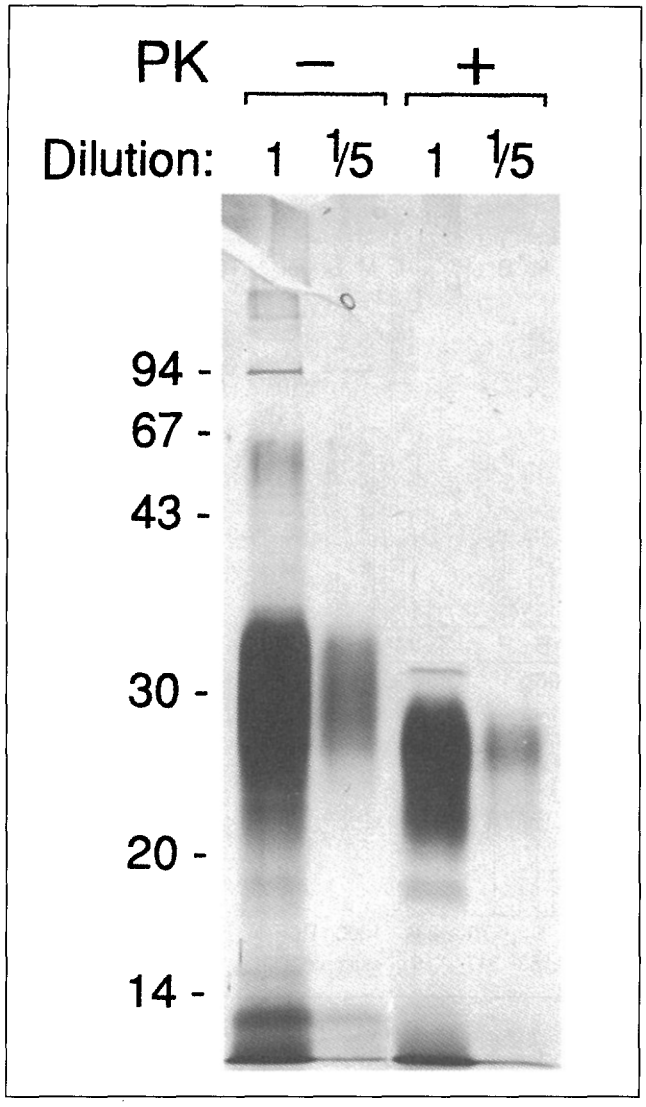

Fig. 5. SDS-PAGE with silver staining of PrP^{Sc} before and after treatment with PK as described in Materials and methods. The thin band seen just above 30 kDa in the third lane was probably PK itself. A 1/5 dilution of the starting material is shown for comparison. Molecular weight markers are indicated at the left in kDa.

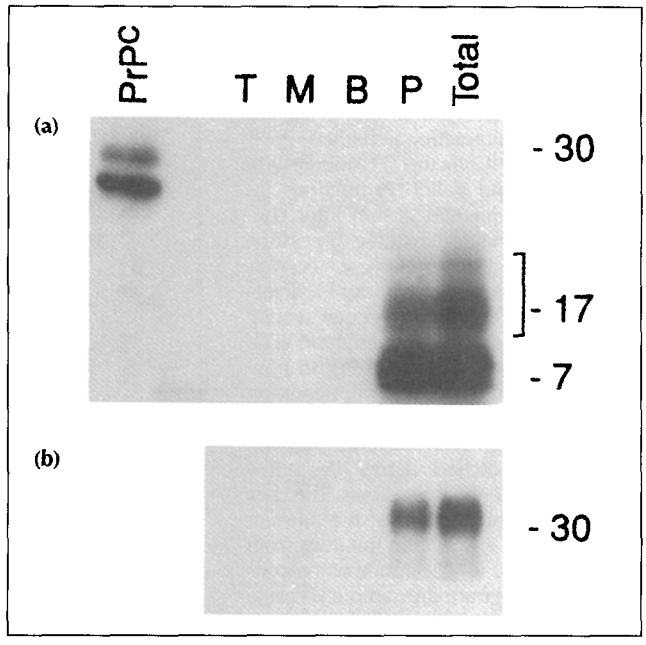

Fig. 6. Both the converting activity and all of the remaining PrP^{Sc} sediment after PK treatment. PrP^{Sc} was treated with PK as described in Materials and methods, incubated at 1 mg ml^{-1} for 5 h at 37 °C in 3 M GdnHCl and fractionated at 234 000 g max on a gradient identical to those described in Figure 4. **(a)** Converting activity (as described in the legend to Fig. 2a) in unfractionated (total) PK-treated PrP^{Sc} in 2.5 M GdnHCl or top (T), middle (M), bottom (B), and pellet (P) fractions. One third of the ^{35}S PrP^{C} used in each conversion reaction is shown without PK digestion in the PrP^{C} lane. **(b)** Immunoblot of the total PrP in the fractions described in (a). Molecular weight markers are indicated at the right in kDa.

range in size from being at least several times larger than solubilized PrP to macroscopic particles. The sedimentation and filtration data provide complementary information about the sizes of species with converting activity. The sedimentation rate of a particle is a function of both its size and shape. Thus, one might argue that subtle differences in sedimentation of PrP species could be explained by differences in conformation rather than aggregation state and that converting activity is associated with a more compact, rapidly sedimenting conformer. If this were the case, however, the more compact conformer would also be expected to pass more readily through the pores of an ultrafiltration membrane than a more extended conformer with a larger Stoke's radius. The opposite result was observed, which is consistent only with the converting activity being associated with an aggregate of larger mass than the solubilized PrP. This conclusion was confirmed by the observation that the detectable converting activity sediments faster than other molecules up to 50 times greater in molecular weight than monomeric PrP.

The nature and origin of the PrP without converting activity that was solubilized from the original PrP^{Sc} aggregate with GdnHCl is not clear, but GdnHCl-soluble subfractions of PrP^{Sc} have also been observed by other investigators [23,24]. Since these PrP molecules appear to be more sensitive to PK than the residual PrP 27–30 aggregate (see Fig. 6), they may be PrP^{C} molecules that are bound (normally or artifactually) to PrP^{Sc} without being fully integrated and converted to the PK-resistant state characterized by PrP 27–30. The stimulation of converting activity by the GdnHCl treatments of PrP^{Sc} [17] may be due to the removal of these PrP molecules which may block access to active catalytic surfaces for the conversion reaction. The presence of these GdnHCl-soluble PrP molecules might also contribute substantially to the PrP^{C} precursor concentration once the GdnHCl is diluted for the conversion reaction.

Ramifications regarding models of PrP^{Sc} formation

Evidence of the sizes of species with converting activity is useful in discriminating between various theories for the mechanism of PrP^{Sc} formation. The observation that a wide range of PrP aggregates possess converting

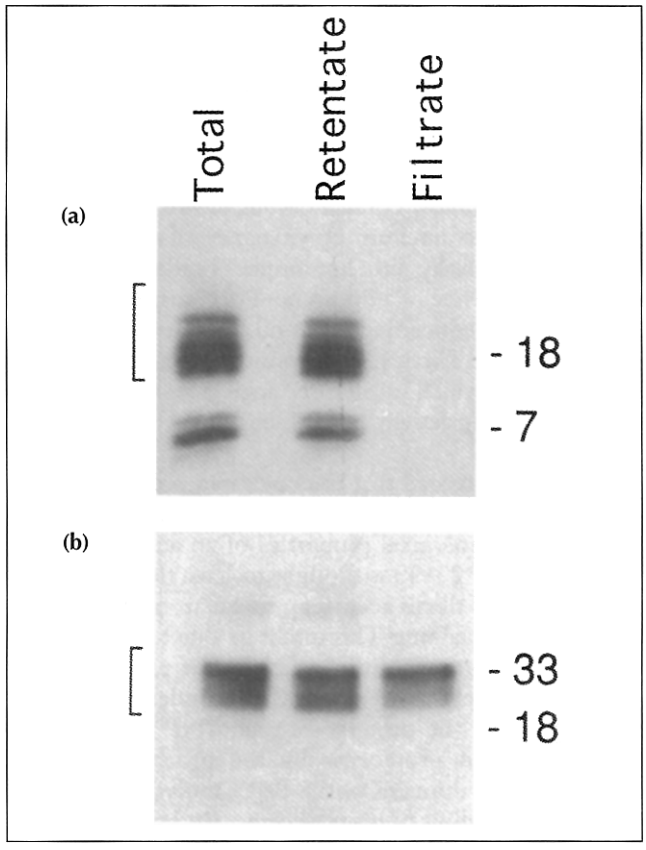

Fig. 7. Ultrafiltration separates solubilized PrP^{Sc} from converting activity. PrP^{Sc} in 3 M GdnHCl was filtered through a 300 kDa NMWL filter as described in Materials and methods. **(a)** Converting activity in equivalent aliquots of the retentate, filtrate and unfractionated sample (total). **(b)** Immunoblot of the total PrP in same fractions. Molecular weight markers are indicated at the right in kDa.

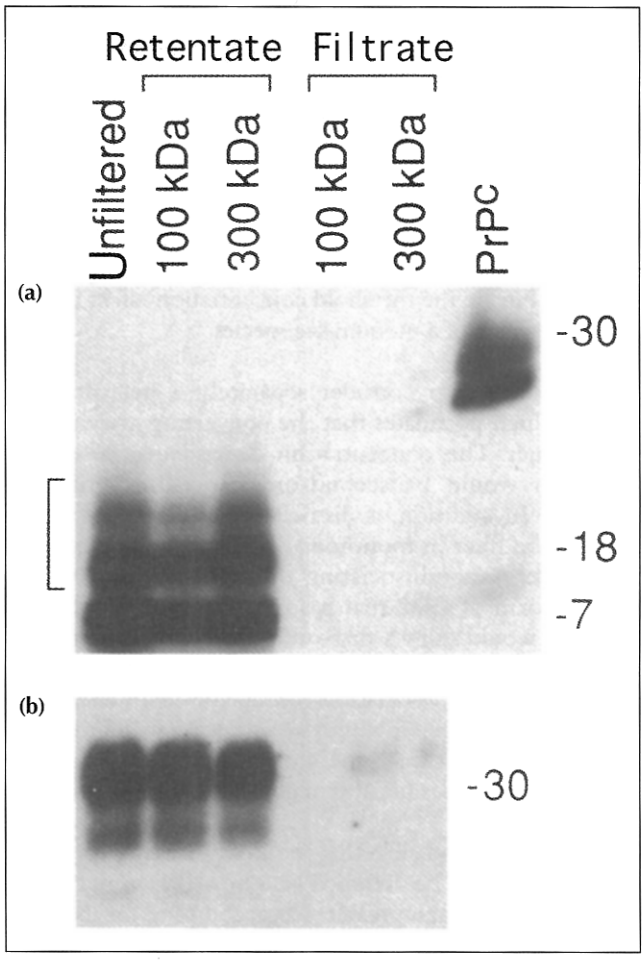

Fig. 8. The PrP^{Sc} and converting activity remaining after PK treatment is retained upon ultrafiltration. The PK-treated PrP^{Sc} described in Figure 6 was incubated in 3 M GdnHCl at a concentration of 1 mg ml^{-1} and filtered as described in Figure 7 except that 100 kDa NMWL filters were also used. **(a)** Converting activity in equivalent aliquots of the indicated fractions. One third of the ^{35}S PrP^{C} used in each conversion reaction is shown without PK digestion in the PrP^{C} lane. **(b)** Immunoblot of the total PrP in the same fractions. Molecular weight markers are indicated at the right in kDa.

activity is consistent with the nucleation model. As in the case of amyloid formation, any aggregate larger than the critical nucleus would be a competent seed for polymerization [21].

The observation of a threshold concentration for converting activity is also consistent with the nucleation proposal, in which the converting activity is a seed for the ordered aggregation of PrP. The threshold concentration may correspond to the critical concentration which is observed for protein polymerization processes known to occur via a nucleation-dependent mechanism (e.g., microtubule formation, flagellum formation, sickle cell fibril formation) [26-29]. Below the critical concentration, the predominant species is the monomer. The nucleus is, by definition, the highest-energy species along the polymerization pathway and the smallest possible seed for polymerization [21]. Since the nucleus is almost completely dissociated below the critical concentration, one would not expect to see conversion. Our attempts to observe conversion below the reported threshold concentration were unsuccessful. Above the critical concentration, the predominant species are large aggregates, in equilibrium with the monomer. All of these post-nucleus aggregates are, in theory, able to seed polymerization. The non-first-order concentration dependence seen at high concentrations of PrP^{Sc} may be due to ultrastructural effects, for example, fibril bundling, which may occur in those concentration ranges. Bundling could decrease the specific activity of the seed by blocking the active growth faces [21]. The threshold concentration observed (~150 nM) may reflect the very low solubility of PrP^{Sc} under the conditions of the *in vitro* conversion reaction (0.75 M GdnHCl). The solubility of PrP^{Sc} might be much lower under more physiological conditions, allowing for further dilution of PrP^{Sc} before activity is lost.

Although PrP^{Sc} is usually isolated in rapidly sedimenting aggregates, it has been suggested that the aggregation of PrP^{Sc} may be largely an artifact of purification and that the active species is a PrP^{Sc} monomer (heterodimer model) that dissociates as a discrete unit from the aggregate [16].

The cell-free conversion assay has given us the opportunity to test directly for converting activity in subfractions of PrP^{Sc} preparations treated with a wide range of conditions (from 0 to 3 M GdnHCl) with varying tendencies to solubilize PrP from the preexisting PrP^{Sc} aggregate. In all cases, converting activity was detected only in the aggregate fractions, and not in supernatants or filtrates containing dissociated PrP^{Sc}. These data are inconsistent with the idea that the active PrP^{Sc} species is solely a monomer or small oligomer. Finally, the threshold concentration effect would not be expected of a monomeric species.

It is instructive to consider separately a heterotrimer model, which postulates that the converting activity is a PrP^{Sc} dimer. The concentration-dependence of dimer formation would be second-order, not first-order as observed. In addition, a dissociating dimer could pass through the filter in monomeric form and reassociate in the filtrate. A nondissociating dimer, analogous to the dimeric form of CD2 that has recently been characterized [30], would show a first-order concentration dependence, but not a threshold concentration. A dimer with an extremely high association equilibrium constant could produce a curve resembling the one seen in Figure 2d; however, it is clear from the sedimentation experiments that a PrP^{Sc} dimer is not the major converting species.

It is theoretically possible that the PrP^{Sc}-derived converting activity could be attached to a non-PrP molecule(s) or aggregate of much greater size, accounting for its sedimentation and filtration properties. Although the complete composition of these aggregates is not clear, silver stain and immunoblotting analyses of fractions containing converting activity indicate that PrP^{Sc} is the predominant protein component, especially after PK digestion (Fig. 5) [25]. Therefore, the particulate behavior of the converting activity is probably due to PrP^{Sc} aggregates, not to PrP^{Sc} monomers bound to a much larger mass of other molecules. This does not eliminate the possibility that some non-PrP molecules have gone undetected or could be minor constituents of the aggregates. This is especially plausible because of the vast excess of PrP^{Sc} over ^{35}S PrP^{C} in the present conversion reaction. For instance, glycosaminoglycans and other possible ligands may be important in the formation or stabilization of PrP^{Sc} [31-34]. These factors might be present in the PrP^{Sc} preparations at substoichiometric levels and may form part of the conversion mechanism. From the present study, we conclude that any such factor must co-purify with GdnHCl-resistant PrP^{Sc} aggregates and be resistant to PK.

Reconciling the properties of the *in vitro* converting activity with those of the scrapie infectious agent

Given the hypothesis that the activity that induces PrP^{Sc} formation is the infectious agent of scrapie, it is relevant to consider how the aggregated nature of the *in vitro* converting activity compares to previous analyses of the size of the scrapie agent. Many studies have indicated that scrapie and Creutzfeldt–Jakob disease infectivity is associated with large sedimentable (>40 S) particles (for review, see [24,35]). But other analyses have indicated that much smaller sized particles can be infectious [36–38]. For instance, scrapie-associated fibrils (SAF) or prion rods are not visible by electron microscopy in all infectious preparations (e.g., liposome preparations) [36,39]. It is possible, however, that the low concentrations of small PrP aggregates required to nucleate polymerization might escape detection, especially in liposomes. Furthermore, the increased infectivity of a liposome–PrP^{Sc} suspension relative to a sample containing the same amount of PrP in the form of amyloid fibrils [39] is consistent with the nucleation model in which smaller PrP aggregates would have a higher converting activity per PrP molecule.

It must be emphasized that the nucleated polymerization model requires only that the seed be ordered, not that it have the morphological properties of an amyloid fibril. In fact, only PrP 27–30 is thought to have the characteristics of amyloid fibrils according to electron microscopy and Congo red staining. This might be due to a reorganization of the structure into a fibril after proteolysis. It seems more likely, however, that the underlying polymeric structure of protease-resistant PrP^{Sc} might be masked prior to proteolysis by the protease-sensitive amino-terminal domains of the PrP^{Sc} molecules, or by a less ordered binding of protease-sensitive PrP molecules to the surface of the polymer. The latter possibility is supported by the loss of a large proportion of the total PrP content in our PrP^{Sc} preparation after PK treatment (Fig 5). These PK-sensitive PrP molecules seem to be the same as those that are effectively solubilized away from the converting activity by 2.5–3 M GdnHCl, since no solubilization of PrP was observed after PK treatment of PrP^{Sc} (Figs. 6, 8).

The sensitivity of the scrapie agent to inactivation by ionizing radiation is consistent with the agent being a PrP dimer of ~55 kDa [37]. It is also consistent with the agent being substantially larger, however. Many oligomeric enzymes have produced monomeric target sizes, indicating that energy transfer between subunits does not occur and that the activity of each subunit can be independent of the activity of its neighbors in the oligomer [40–42]. Similarly, if the scrapie agent is an aggregate of PrP, the interpretation of the radiation target size data will be complicated by the fact that a multimeric PrP seed may be resistant to radiation damage of subunits that are not part of the growth face. The observed target size of 55 kDa may reflect a growth face defined by two PrP molecules within the context of a larger polymer.

Significance

The scrapie infectious agent may consist solely of a structural isomer of a normal cellular protein (prion protein, PrP). The molecular mechanism of scrapie infection remains a mystery, however, largely due to the difficulties associated with

designing unambiguous *in vivo* experiments. We have developed an *in vitro* model, which has several key properties that appear related to scrapie infection. This paper reports the initial characterization of the scrapie-brain-derived species ('converting activity') which is responsible for *in vitro* conversion of the cellular prion protein (PrP^C) into a form which is biochemically indistinguishable from the scrapie-specific form, PrP^{Sc}. The converting activity required a threshold concentration of PrP^{Sc}, but was separated from soluble PrP by ultrafiltration and centrifugation. Sedimentation analysis demonstrated that the converting activity was associated with high molecular weight aggregates of PrP. These data are consistent with a mechanism of conversion that resembles a crystallization process in that it is rate-limited by nucleus formation and accelerated by seeding. The nucleation mechanism is known to operate in the assembly of cytoskeletal components such as microtubules and pathological assemblies such as sickle cell fibrils and amyloid fibrils. Future experiments will be aimed at determining whether this mechanism is operative *in vivo*. If that can be demonstrated, it may have implications for the etiology and treatment of the transmissible spongiform encephalopathies.

Materials and methods

PrP^{Sc}

PrP^{Sc} was purified from the brains of hamsters infected with the 263K strain of scrapie as described [17,25] and was sonicated into 0.5–1% sulfobetaine 3-14 in phosphate buffered saline (PBS; 20 mM sodium phosphate and 130 mM NaCl, pH 7.4) and stored at –20 °C prior to use.

In some experiments, PrP^{Sc} was treated with PK prior to fractionation as follows. PrP^{Sc} at a concentration of 200 μg ml^{-1} in 10% (w/v) NaCl, 1% sulfobetaine 3-14 in TEND (10 mM Tris-HCl, pH 8.3, 1 mM EDTA, 1 mM dithiothreitol (DTT) and 130 mM NaCl) was treated with 25 μg ml^{-1} PK for 1 h at 37 °C. The reaction was stopped by adding aprotinin, leupeptin, and Pefabloc to 1.5 μM, 10 μM, and 1 mM, respectively. The PrP^{Sc} was centrifuged for 15 min at 12,000 g at 4 °C and the supernatant removed. The pellet was sonicated into 0.1% sarkosyl, 0.01 μM aprotinin and 1 μM leupeptin, and the centrifugation repeated. The resultant pellet was sonicated into 1% sulfobetaine 3-14 and PBS and stored at –20 °C until use.

^{35}S-PrP^C

The recombinant hamster PrP^C used in this study was designed to contain all but the carboxy-terminal residue (Ser231) of the mature hamster PrP^C. This protein will therefore lack the glycophosphatidyl inositol (GPI) anchor [17], which is normally attached to Ser231 [43]. We have found this construct to be the one most efficiently labeled and converted to protease-resistant forms with hamster PrP^{Sc} in the cell-free conversion reaction. This construct was made by converting codon 231 to a stop codon in the hamster PrP gene [17], eliminating the codons encoding Ser231 and the carboxy-terminal GPI signal sequence (residues 232–254) that is removed during normal biosynthesis [43]. This gene was cloned into a pSFF retroviral expression vector and expressed in mouse fibroblast cells by standard techniques [44].

A subclone of these fibroblasts was preincubated in methionine and cysteine-deficient minimal Eagle's medium (MEM, supplemented with 1% dialyzed fetal bovine serum) for 1 h and incubated with the label (~1 mCi ^{35}S methionine/cysteine (Expre$^{35}S^{35}S$ label, New England Nuclear) per 25-cm^2 flask of 60–80% confluent cells) for 90–120 min in this same medium. The cells were then washed and lysed in ice-cold lysing buffer (LB) containing 0.5% Triton X-100 and 0.5% sodium deoxycholate (1 ml per 25-cm^2 flask). The lysates were cleared by centrifugation for 5 min at 1000 g at 4 °C, and the proteins precipitated with four volumes of methanol at –20 °C for ≥ 1 h. The precipitated proteins were resuspended by cuphorn sonication into DLPC buffer (0.05 M Tris-HCl, pH 8.2, 0.15 M NaCl, 2% (w/v) N-lauryl sarcosine, 0.4% (w/v) L-α-lecithin (from egg yolk)) [9]. The quantity of DLPC buffer used was 1 ml per 25-cm^2 flask equivalent of cell proteins. Hamster PrP-specific monoclonal antibody 3F4 [45] was incubated with the suspension (2.5 μl ascites ml^{-1} DLPC) overnight at 4 °C, and antibody–antigen complexes were collected by binding to protein A Sepharose beads (10 μl of 10% w/v suspension per μl of antibody). After washing the beads with DLPC buffer and then 1% N-laurylsarcosine, 500 mM NaCl, 50 mM Tris-HCl, pH 7.0 at 4 °C, the residual liquid was drawn off the bead pellet with a Hamilton syringe and the PrP was eluted in 25 μl of 3 M GdnHCl per 5 mg dry weight equivalent of beads. The beads were agitated in the eluant for 15 min at 37 °C. The eluate was drawn off the beads, and the elution step repeated with fresh eluant. The eluates were stored on ice up to several weeks prior to use with no detectable degradation of PrP^C.

Cell-free conversion reaction

Aliquots (2 μl) of samples to be assayed for converting activity were mixed with 2 μl of ^{35}S PrP^C (60 000 counts per minute (cpm)) in 3 M GdnHCl (estimated by semi-quantitative immunoblotting to be ~5–10 ng total PrP^C per 60 000 cpm of ^{35}S PrP^C). This mixture was diluted with 12 μl of 2 mM cetyl pyridinium chloride, 50 mM sodium citrate–HCl, pH 6.4 (CPC-Cit) at 20 °C and incubated at 37 °C for 2–45 h. The mixture was diluted further with 64 μl of 130 mM NaCl, 50 mM Tris-HCl, pH 7.4 (at 20 °C) (TN). Then 2 μl of 1 mg ml^{-1} PK was added to give a final concentration of 25 μg ml^{-1}. This mixture was incubated at 37 °C for 1 h. The PK was then inhibited by adding 24 μg Pefabloc (Boehringer-Mannheim) and 10 μg of thyroglobulin (carrier protein). Methanol (four volumes at –20 °C) was added to precipitate the remaining proteins. The precipitate was collected by centrifugation and subjected to SDS-PAGE on 14% acrylamide Novex precast gels. Radioactive proteins were detected in the gels by fluorography with Entensify (DuPont) or with a Phosphorimager (Molecular Dynamics). The Phosphorimager was used to quantify PK-resistant ^{35}S-labelled bands and to compare their radioactivity with that of the of ^{35}S PrP^C precursor bands.

Centrifugation of PrP^{Sc}

For the simple centrifugation of GdnHCl-treated PrP^{Sc} (as in Fig. 3), 50 μl of PrP^{Sc}, pretreated in 3 M GdnHCl at 1 mg ml^{-1} for 5 h at 37 °C, was centrifuged at 70 000 rpm for 50 min at 20 °C in a Beckman TL100.1 rotor. The supernatant was collected and the pellet was resuspended by cuphorn sonication into 50 μl of fresh 3 M GdnHCl. Aliquots of each fraction were assayed for converting activity in the cell-free conversion

reaction described above, and for total PrP content by immunoblotting as described below.

Sedimentation velocity gradients were performed by layering 20 µl of a given PrP^{Sc} preparation (preincubated at 37 °C for 2–18 h in 2.5 M GdnHCl) over 40 µl of a solution with identical GdnHCl concentration and 5% (w/v) sucrose in a Beckman 7 x 20 mm polycarbonate centrifuge tube. The tubes were spun to give the designated maximum g-force for 30 min at 20 °C in a Beckman TLS 55 swinging bucket rotor using the slowest acceleration and deceleration settings. The gradients were fractionated as shown in Figure 4 and the pellet was sonicated into an additional 20 µl of solution. Equal aliquots of the fractions were assayed for converting activity and for total PrP content by immunoblotting. Molecular weight standard proteins were dissolved in 2.5 M GdnHCl at ~1 mg ml^{-1} and fractionated on gradients exactly as was PrP^{Sc}. The concentrations of the molecular weight standards in the fractions were determined by SDS-PAGE with silver staining, except in the cases of thyroglobulin and blue dextran. These proteins were too large to enter the SDS-PAGE gels; they were run on separate gradients and their concentrations in the fractions were determined by absorbance at 280 nm and 625 nm, respectively.

Estimation of sedimentation coefficients

The sedimentation coefficient (s, in Svedberg units) of particles expected to be 90% cleared from the sedimentation velocity gradient sample zones within the time of centrifugation (t in h) was estimated using the following equation (Beckman centrifuge manual):

$$s_{obs} = k/t$$

where k is the clearing factor for the sample zone given by

$$k = 253303 \ln (r_{max}/r_{min})/(RPM/1000)^2$$

where r_{max} and r_{min} are the maximum and minimum radii, respectively, of the sample zone within the spinning rotor and RPM is the revolutions per minute of the rotor.

Estimates of the $s_{20,w}$ values (s at 20 °C in water) for the particles were obtained from s_{obs} using equation (2) of Prusiner, *et al.* [46] to correct for the difference in density between 2.5 M GdnHCl and water. No correction for a difference in viscosity was made.

Ultrafiltration of PrP^{Sc}

Millipore Ultrafree-MC polysulfone membrane 100 000 and 300 000 NMWL filter units were used according to the manufacturer's instructions. PrP^{Sc} to be filtered was first incubated in 3 M GdnHCl at 37 °C at 1 mg ml^{-1} for 2–5 h. 50 µl of the PrP^{Sc} solution was loaded onto the filter and then centrifuged at 1–2000 rpm until about half of the solution had been filtered. The retentate fractions were then diluted back to 50 µl with 3 M GdnHCl (the filtrates were left neat) and 2 µl of each was immediately added to a conversion reaction to assess converting activity. Equivalent parts of each fraction were also diluted and immunoblotted to determine the total PrP content. After an initial protease treatment, PK-treated PrP^{Sc} was filtered and assayed identically to non-protease-treated PrP^{Sc}.

Immunoblotting

SDS-PAGE was performed using 20% acrylamide PhastSystem gels (Pharmacia) (Figs. 3b, 7b) or Novex 14% acrylamide precast gels (all other figures). Gels were immunoblotted onto a PVDF Immobilon-P (Millipore) membrane using the PhastSystem blotter or a Milliblot-SDE transfer system (Millipore). The membranes were blocked using 5% nonfat dry milk in 0.05% Tween 20, 150 mM NaCl, 10 mM Tris-HCl, pH 8.0 (TBST) and incubated with a polyclonal rabbit antibody to a synthetic peptide corresponding to hamster PrP residues 90–104 [47] (1:2000 in TBST) at room temperature for 1 h. After washing, an anti-rabbit immunoglobulin, horseradish peroxidase-linked antibody (Amersham) was incubated with the membranes for 30 min. The membranes were then washed and developed with ECL chemiluminescence detection kit (Amersham).

Acknowledgements: We thank Bob Evans and Gary Hettrick for graphics assistance, and Drs Suzette Priola, Richard Bessen, John Portis and Richard Race for critical review of this manuscript. This work was supported in part by a National Science Foundation Presidential Young Investigator Award with matching funds from the Genentech and Merck Corporations.

References

1. Pocchiari, M. (1994). Prions and related neurological diseases. *Mol. Aspects Med.* **15**, 195–291.
2. Bolton, D.C., McKinley, M.P. & Prusiner, S.B. (1982). Identification of a protein that purifies with the scrapie prion. *Science* **218**, 1309–1311.
3. Diringer, H., Gelderblom, H., Hilmert, H., Ozel, M., Edelbluth, C. & Kimberlin, R.H. (1983). Scrapie infectivity, fibrils and low molecular weight protein. *Nature* **306**, 476–478.
4. Prusiner, S.B., *et al.*, & Glenner, G.G. (1983). Scrapie prions aggregate to form amyloid-like birefringent rods. *Cell* **35**, 349–358.
5. Oesch, B., *et al.*, & Weissmann, C. (1985). A cellular gene encodes scrapie PrP 27–30 protein. *Cell* **40**, 735–746.
6. Hope, J., Morton, L.J.D., Farquhar, C.F., Multhaup, G., Beyreuther, K. & Kimberlin, R.H. (1986). The major polypeptide of scrapie-associated fibrils (SAF) has the same size, charge distribution and N-terminal protein sequence as predicted for the normal brain protein (PrP). *EMBO J.* **5**, 2591–2597.
7. Meyer, R.K., McKinley, M.P., Bowman, K.A., Braunfeld, M.B., Barry, R.A. & Prusiner, S.B. (1986). Separation and properties of cellular and scrapie prion protein. *Proc. Natl. Acad. Sci. USA* **83**, 2310–2314.
8. Rubenstein, R., *et al.*, & Wisniewski, H.M. (1986). Detection of scrapie-associated fibril (SAF) proteins using anti-SAF antibody in non-purified tissue preparations. *J. Gen. Virol.* **67**, 671–681.
9. Borchelt, D.R., Scott, M., Taraboulos, A., Stahl, N. & Prusiner, S.B. (1990). Scrapie and cellular prion proteins differ in the kinetics of synthesis and topology in cultured cells. *J. Cell Biol.* **110**, 743–752.
10. Caughey, B. & Raymond, G.J. (1991). The scrapie-associated form of PrP is made from a cell surface precursor that is both protease- and phospholipase-sensitive. *J. Biol. Chem.* **266**, 18217–18223.
11. Stahl, N., *et al.*, & Prusiner, S.B. (1993). Structural studies of the scrapie prion protein using mass spectrometry and amino acid sequencing. *Biochemistry* **32**, 1991–2002.
12. McKinley, M.P., Bolton, D.C. & Prusiner, S.B. (1983). A protease-resistant protein is a structural component of the scrapie prion. *Cell* **35**, 57–62.
13. Caughey, B., Ernst, D. & Race, R.E. (1993). Congo red inhibition of scrapie agent replication. *J. Virol.* **67**, 6270–6272.
14. Griffith, J.S. (1967). Self-replication and scrapie. *Nature* **215**, 1043–1044.
15. Bolton, D.C. & Bendheim, P.E. (1988). A modified host protein model of scrapie. In *Novel Infectious Agents and the Central Nervous System.* (Bock, G. & Marsh, J. , eds.), pp. 164–181, John Wiley & Sons, Chichester.
16. Prusiner, S.B. (1991). Molecular biology of prion diseases. *Science* **252**, 1515–1522.
17. Kocisko, D.A., *et al.*, & Caughey, B. (1994). Cell-free formation of protease-resistant prion protein. *Nature* **370**, 471–474.
18. Kocisko, D.A., Priola, S.A., Raymond, G.J., Chesebro, B., Lansbury, P.T., Jr. & Caughey, B. (1995). Species specificity in the cell-free conversion of prion protein to protease-resistant forms: a model for the scrapie species barrier. *Proc. Natl. Acad. Sci. USA* **92**, 3923–3927.
19. Bessen, R.A., Kocisko, D.A., Raymond, G.J., Nandan, S., Lansbury, P.T., Jr. & Caughey, B. (1995). Nongenetic propagation of strain-specific

properties of scrapie prion protein. *Nature* **375**, 698–700.
20. Brown, P., Goldfarb, L.G. & Gajdusek, D.C. (1991). The new biology of spongiform encephalopathy: infectious amyloidoses with a genetic twist. *Lancet* **337**, 1019–1022.
21. Jarrett, J.T. & Lansbury, P.T., Jr. (1993). Seeding 'one-dimensional crystallization' of amyloid: a pathogenic mechanism in Alzheimer's disease and scrapie? *Cell* **73**, 1055–1058.
22. Rogers, M., Yehiely, F., Scott, M. & Prusiner, S.B. (1993). Conversion of truncated and elongated prion proteins into the scrapie isoform in cultured cells. *Proc. Natl. Acad. Sci. USA* **90**, 3182–3186.
23. Safar, J., Roller, P.P., Gajdusek, D.C. & Gibbs, C.J., Jr. (1993). Conformational transitions, dissociation, and unfolding of scrapie amyloid (prion) protein. *J. Biol. Chem.* **268**, 20276–20284.
24. Manuelidis, L., Sklaviadis, T., Akowitz, A. & Fritch, W. (1995). Viral particles are required for infection in neurodegenerative Creutzfeld–Jakob disease. *Proc. Natl. Acad. Sci. USA* **92**, 5124–5128.
25. Caughey, B.W., Dong, A., Bhat, K.S., Ernst, D., Hayes, S.F. & Caughey, W.S. (1991). Secondary structure analysis of the scrapie-associated protein PrP 27–30 in water by infrared spectroscopy. *Biochemistry* **30**, 7672–7680.
26. Gaskin, F. & Cantor, C.R. (1974). Turbidimetric studies of the *in vitro* assembly and disassembly of porcine neurotubules. *J. Mol. Biol.* **89**, 737–758.
27. Andreu, J.M. & Timasheff, S.N. (1986). The measurement of cooperative protein self-assembly by turbidity and other techniques. *Methods Enzymol.* **130**, 47–59.
28. Asakura, S. (1970). Polymerization of flagellin and polymorphism of flagella. *Adv. Biophys.* **1**, 99–155.
29. Eaton, W.A. & Hofrichter, J. (1990). Sickle cell hemoglobin polymerization. *Adv. Protein Chem.* **40**, 63–279.
30. Murray, A.J., Lewis, S.J., Barclay, A.N. & Brady, R.L. (1995). One sequence, two folds: a metastable structure of CD2. *Proc. Natl. Acad. Sci. USA* **92**, 7337–7341.
31. Snow, A.D., *et al.*, & Prusiner, S.B. (1990). Immunolocalization of heparan sulfate proteoglycans to the prion protein amyloid plaques of Gerstmann–Straussler syndrome, Creutzfeldt–Jakob disease and scrapie. *Lab. Invest.* **63**, 601–611.
32. Caughey, B., Brown, K., Raymond, G.J., Katzenstein, G.E. & Thresher, W. (1994). Binding of the protease-sensitive form of PrP (prion protein) to sulfated glycosaminoglycan and Congo red. *J. Virol.* **68**, 2135–2141.
33. Aiken, J.M. & Marsh, R.F. (1990). The search for scrapie agent nucleic acid. *Microbiol. Rev.* **54**, 242–246.
34. Riesner, D. (1991). The search for a nucleic acid component of scrapie infectivity. *Sem. Virol.* **2**, 215–226.
35. Rohwer, R.G. (1991). The scrapie agent: 'a virus by any other name'. *Curr. Top. Microbiol. Immunol.* **172**, 195–232.
36. Gabizon, R., McKinley, M.P., Groth, D.F., Kenaga, L. & Prusiner, S.B. (1988). Properties of scrapie prion protein liposomes. *J. Biol. Chem.* **263**, 4950–4955.
37. Bellinger-Kawahara, C.G., Kempner, E., Groth, D., Gabizon, R. & Prusiner, S.B. (1988). Scrapie prion liposomes and rods exhibit target sizes of 55,000 Da. *Virology* **164**, 537–541.
38. Safar, J., *et al.*, & Gibbs, C.J., Jr. (1990). Molecular mass, biochemical composition, and physicochemical behavior of the infectious form of the scrapie precursor protein monomer. *Proc. Natl. Acad. Sci. USA* **87**, 6373–6377.
39. Gabizon, R., McKinley, M.P. & Prusiner, S.B. (1987). Purified prion proteins and scrapie infectivity copartition into liposomes. *Proc. Natl. Acad. Sci. USA* **84**, 4017–4021.
40. Kempner, E.S. & Miller, J.H. (1983). Radiation inactivation of glutamate dehydrogenase hexamer: lack of energy transfer between subunits. *Science* **222**, 586–589.
41. Harmon, J.T., Nielson, T.B. & Kempner, E.S. (1985). Molecular weight determinations from radiation inactivation. *Methods Enzymol.* **117**, 65–94.
42. Harmon, J.T., Kahn, C.R., Kempner, E.S. & Schlegel, W. (1980). Characterization of the insulin receptor in its membrane environment by radiation inactivation. *J. Biol. Chem.* **255**, 3412–3419.
43. Stahl, N., Baldwin, M.A., Burlingame, A.L. & Prusiner, S.B. (1990). Identification of glycoinositol-phospholipid-linked and truncated forms of the scrapie prion protein. *Biochemistry* **29**, 8879–8884.
44. Chesebro, B., Wehrly, K., Caughey, B., Nishio, J., Ernst, D. & Race, R. (1993). Foreign PrP expression and scrapie infection in tissue culture cell lines. *Dev. Biol. Stand.* **80**, 131–140.
45. Kascsak, R.J., *et al.*, & Diringer, H. (1987). Mouse polyclonal and monoclonal antibody to scrapie-associated fibril proteins. *J. Virol.* **61**, 3688–3693.
46. Prusiner, S.B., Hadlow, W.J., Eklund, C.M., Race, R.E. & Cochran, S.P. (1978). Sedimentation characteristics of the scrapie agent from murine spleen and brain. *Biochemistry* **17**, 4987–4992.
47. Caughey, B., Raymond, G.J., Ernst, D. & Race, R.E. (1991). N-terminal truncation of the scrapie-associated form of PrP by lysosomal protease(s): implications regarding the site of conversion of PrP to the protease-resistant state. *J. Virol.* **65**, 6597–6603.

Received: **23 October 1995.** Accepted: **31 October 1995.**